A MULTI-ZONAL LOCAL SOLUTION METHODOLOGY FOR THE ACCELERATED SOLUTION OF THE TURBULENT NAVIER-STOKES EQUATIONS

D. Drikakis and S. Tsangaris

Laboratory of Aerodynamic N.T.U.A.
P.O. Box 640 70, 157 10 Zografou-Athens, Greeece

Abstract

A multi-zonal local solution method is developed for the solution of the compressible Navier-Stokes equations. The main feature of the method is the coupling of the Navier-Stokes equations with the Euler equations and the local adaptive mesh solution procedure. The methodology is applied to turbulent flow fields past an airfoil. A Flux Vector Splitting method with an upwind scheme up to the fourth order of accuracy is used for the discretization of the inviscid fluxes. The system of equations is solved by an unfactored implicit method using Gauss-Seidel relaxation. The multizonal local solution method gives more rapid convergence to the steady state solution retaining the accuracy of the computational code.

Introduction

Technological improvements in supercomputer speed and memory size provided the means to solve the full compressible Navier-Stokes equations for turbulent flow fields and complex geometries. However, large amounts of computer time are required for the solution of the equations especially for problems in design practice. In order to reduce the computational time a multi-zonal local solution method (LSM) is presented for the solution of the Navier-Stokes equations in high Reynolds number flows.

In the past, other authors have developed zonal methods [1-4] coupling, different kind of equations in discrete regions of the flow field. In [1] Navier-Stokes equations are solved near the wall and Euler equations elsewhere. Van Dalsem and Steger [2] have used a combination of a Navier-Stokes solution on a coarse mesh and a boundary-layer solution on a fine mesh. Schmatz [3] has developed a coupling of the Euler and the Navier-Stokes equations with the boundary layer equations. Reduction of the computational time is obtained by solving the Navier-Stokes equations only in the region of the flow field where strong viscous interactions occur. Extension of this method in three dimensional flows can be found in [4].

The contribution of the present work is the development of a multi-zonal local methodology which combines the numerical techniques of the Local Solution and the mesh sequencing with the coupling of the Navier-Stokes and Euler equations. A local solution method was been developed in the past [5] for inviscid and laminar flow fields. This method uses, initially, a sequence of coarser meshes in order to provide a better initial guess for the solution on the fine mesh. Local solution is obtained in discrete regions (partial meshes) of the flow field during the convergence to the steady state solution. The above procedure is extended in the present work to turbulent flow fields while Navier-Stokes equations are solved near the wall and Euler equations elsewhere. Reduction of the computational time is obtained from the zonal procedure as well as from the local solution and the mesh sequencing techniques.

The above procedure has been developed on a Navier-Stokes Code [6] which uses a modified Steger-Warming Flux Vector Splitting method [7] for the discretization of the inviscid fluxes and the Chakravarthy's scheme [8] for the discretization of the viscous fluxes. An upwind interpolation scheme [9] up to the fourth order of accuracy is used for the calculation of the conservative variables on the cell faces. The system of equations is solved by an unfactored implict method using Gauss-Seidel relaxation sweeps. Implicit treatment of the boundary conditions is obtained by Newton sub-iterations. The multi-zonal local solution methodology is applied to transonic turbulent flow fields past an airfoil.

Governing equations

The governing equations are the time dependent Navier-Stokes equations for a compressible fluid. These equations can be written in conservation dimensionless form and for a generalized coordinate system as :

$$J \cdot U_t + (E_{inv})_\xi + (G_{inv})_\zeta = \frac{1}{Re}\left[\left(E_{vis}\right)_\xi + \left(G_{vis}\right)_\zeta\right] \qquad (1)$$

where Re is the Reynolds number and $U = (\varrho, \varrho u, \varrho w, e)^T$ is the conservative solution unknown vector. E_{inv}, G_{inv} are the inviscid flux vectors while E_{vis}, G_{vis} are the viscous flux vectors. $J = x_\xi z_\zeta - z_\xi x_\zeta$ is the Jacobian coordinates x, z to generalized coordinates ξ, ζ. The inviscid and viscous fluxes are defined as :

$$E_{inv} = J\left(\tilde{E}\xi_x + \tilde{G}\xi_z\right)$$
$$G_{inv} = J\left(\tilde{E}\zeta_x + \tilde{G}\zeta_z\right)$$
$$E_{vis} = J\left(\tilde{R}\xi_x + \tilde{S}\xi_z\right)$$
$$G_{vis} = J\left(\tilde{R}\zeta_x + \tilde{S}\zeta_z\right)$$

with

$$\tilde{E}=\begin{pmatrix}\rho u\\ \rho u^2+p\\ \rho uw\\ (e+p)u\end{pmatrix}\quad,\quad \tilde{G}=\begin{pmatrix}\rho w\\ \rho uw\\ \rho w^2+p\\ (e+p)w\end{pmatrix}$$

$$\tilde{R}=\begin{pmatrix}0\\ \tau_{xx}\\ \tau_{xz}\\ u\tau_{xx}+w\tau_{xz}-q_x\end{pmatrix}\quad,\quad \tilde{S}=\begin{pmatrix}0\\ \tau_{zx}\\ \tau_{zz}\\ u\tau_{xz}+w\tau_{zz}-q_z\end{pmatrix}$$

The indices ξ, ζ denote partial derivatives, except for the stresses τ_{xx}, τ_{xz}, τ_{zx}, τ_{zz} and the heat terms q_x, q_z. The stresses and the heat terms are given as :

$$\tau_{xx}=-p-\frac{2}{3}\mu\,(-2u_x+w_z)$$

$$\tau_{zz}=-p-\frac{2}{3}\mu\,(+u_x-2w_z)$$

$$\tau_{xz}=\tau_{zx}=\mu\,(w_x+u_z)$$

$$q_x=-\frac{\gamma\mu}{Pr}T_x\quad,\quad q_z=-\frac{\gamma\mu}{Pr}T_z$$

where $Pr = \mu c_{p/k}$ is the Prandtl number, ϱ is the density, u and w the velocity components in the x, z directions respectively and e is the total energy. μ, k are the viscosity and the heat conductivity coefficients while T is the gas temperature. Dimensionless viscosity can be defined by Sutherland law :

$$\mu=\frac{110.4/T_o+1}{110.4/T_o+T}\cdot T^{3/2}$$

T_o is the temperature of dimensionalization. The formulation of the governing equations is completed by an equation of state :

$$p = \varrho(\gamma\text{-}1)i$$

where γ is the ratio of specific heats and i the specific internal energy.

Discretization of the inviscid and viscous fluxes

The discretization of the inviscid fluxes is carried out by a modified Steger-Warming Flux Vector Splitting method [5], [9]. The Steger-Warming FVS decomposes the inviscid flux into two parts, positive and negative, in accordance with the sign of the eigenvalues :

$$\left(E_{inv}\right)_{i+\frac{1}{2}}=\left(T\Lambda^{+}T^{-1}\right)_{i+\frac{1}{2}}U^{-}_{i+\frac{1}{2}}+\left(T\Lambda^{-}T^{-1}\right)_{i+\frac{1}{2}}U^{+}_{i+\frac{1}{2}}\qquad(2)$$

where T, T^{-1} are the left and right eigenvectors matrices respectively, while Λ^+ and Λ^- are the positive and negative eigenvalue matrices. The splitted fluxes are defined on the cell faces of the computational volume because this formulation improves the results in the boundary layers, in contrast with the definition of the fluxes on the center of the volume. The eigenvalues in the positive and negative eigenvalue matrices are splitted as :

$$\lambda_0^{\pm}=\frac{\left(\lambda_1^{\pm}+\lambda_2^{\pm}\right)}{2}$$

$$\lambda_j^{\pm}=\frac{\lambda_j\pm|\lambda_j|}{2}\qquad j=1,2$$

where

$$\lambda_0=u\xi_x+w\xi_z\quad,\quad \lambda_1=\lambda_0+s\quad,\quad \lambda_2=\lambda_0-s$$

s represents the speed of sound. The splitted convective fluxes can be defined as

$$\left(E_{inv}\right)^{\pm}_{i+\frac{1}{2}}=\rho|\nabla\xi|\begin{pmatrix}\frac{1}{2}\left(\lambda_1^{\pm}+\lambda_2^{\pm}\right)\\ \left(u+\frac{s\xi_x}{\gamma}\right)\frac{\lambda_1^{\pm}}{2}+\left(u-\frac{s\xi_x}{\gamma}\right)\frac{\lambda_2^{\pm}}{2}\\ \left(w+\frac{s\xi_z}{\gamma}\right)\frac{\lambda_1^{\pm}}{2}+\left(w-\frac{s\xi_z}{2}\right)\frac{\lambda_2^{\pm}}{2}\\ \frac{1}{2}H^{\pm}\left(\lambda_1^{\pm}+\lambda_2^{\pm}\right)\end{pmatrix}$$

with

$$\xi_x=\frac{\xi_x}{\sqrt{\xi_x^2+\xi_z^2}}\quad,\quad \xi_z=\frac{\xi_z}{\sqrt{\xi_x^2+\xi_z^2}}$$

The viscous terms are discretized using central differences for the normal second derivatives and an "upwind" type scheme for the cross derivatives. This scheme was proposed in the past by Chakravarthy [8].

High order extrapolation schemes

The conservative variables on the cell faces are calculated by a hybrid upwind extrapolation scheme up to the fourth order of accuracy. The hybrid scheme is constructed by the superposition of the first, second, third and fourth order extrapolation schemes :

$$U^{\pm}_{i+\frac{1}{2}}=A\cdot U^{1,\pm}+(1-A)\cdot\left\{BU^{2,\pm}+(1-B)\left[CU^{3,\pm}+(1-C)\right]U^{4,\pm}\right\}$$

The superscripts 1, 2, 3, 4 denote the varying order of the extrapolation. For instance the third and the fourth order extrapolation are defined as :

Third order :

$$\left(U^3_{i+\frac{1}{2}}\right)^- = \frac{1}{6}\left(5U_i - U_{i-1} + 2U_{i+1}\right)$$

$$\left(U^3_{i+\frac{1}{2}}\right)^+ = \frac{1}{6}\left(5U_{i+1} - U_{i+2} + 2U_i\right)$$

Forth order :

$$\left(U^4_{i+\frac{1}{2}}\right)^- = \left(U^4_{i+\frac{1}{2}}\right)^+ = \frac{1}{2}\left(7U_i + 7U_{i+1} - U_{i-1} - U_{i+2}\right)$$

The terms A,B are limiter functions and are defined by the second order derivatives of the pressure :

$$A = \min\left(1, d\left|p^2_{\xi\xi,i+1} - p^2_{\xi\xi,i}\right|\right)$$

$$B = \min\left(1, d\left|p^2_{\xi\xi,i+1} - p^2_{\xi\xi,i}\right|\right)$$

The values of the constants d, b, C are d = 4.5, b = 2.5 and C = 2.25.

Zonal modelling

The concept of zonal modelling results from the fact that in high Reynolds number attached flows, diffusion effects are important near the body surface and in bounded shear layers in the wake of the flow field. Thus, in regions distant from the above regions the flow can be considered as inviscid. In regions where the viscous effects are considered important Navier-Stokes equations are solved while Euler equations are solved elsewhere. A schematic representation of the zonal modelling is shown in figure 1 for the turbulent flow over an airfoil. The definition of the viscous zonal boundary is based on the physics of the problem.

The zonal modelling is associated with the mesh sequencing technique and with the local solution of the equations, which are described in the following sections.

Mesh sequencing and local solution techniques have been developed in the past [5, 6] for inviscid and laminar viscous flows. A short description of these techniques and indication of the differences in the turbulent flow applications follow.

Mesh sequencing and local solution techniques for turbulent flows

In the mesh sequencing technique an initial guess on the fine mesh is obtained by first iterating the solution of the equations on a sequence of coarser grids and then interpolating the solution to the next finer grid. The coarse mesh is constructed by eliminating every second line of the fine mesh in each direction. The refining grid criterion for the interpolation of the solution from the coarse to the fine mesh is the maximum variation max ($|\Delta\varrho|$, $|\Delta(\varrho u)|$, $|\Delta(\varrho w)|$, $|\Delta e|$) of the conservative variables during the iterations. The above criterion is also used for turbulent flows. Because in the mesh sequencing procedure the center of the volumes of the fine mesh is not a subset of the volumes of the coarse mesh, bilinear interpolation is used for the calculation of the conservative variables on the fine mesh using the corresponding variables on the coarse mesh.

The local solution technique originates from the nonuniformities of the flow variation towards a steady or unsteady solution. Thus, the local solution of the equations can be applied only in regions where the disturbances are large because in the remaining field the solution has been achieved. The local solution of the equations is obtained in subregions (partial meshes) of the fine mesh characterized by large values of the numerical disturbances. In the case of inviscid or laminar viscous flows the solid boundaries may, or may not be contained in the partial meshes. A typical example is shown in figures (2a, b). In figure (2a) the partial meshes A and B overlap a part of the solid boundary of the airfoil while in figure (2b) partial meshes do not overlap solid boundaries.

In the case of high Reynolds number flows large numerical disturbances are generated in the turbulent boundary layers. These disturbances are eliminated at the same rate around every solid boundary and thus all the solid boundaries must be contained in the partial mesh during the local solution of the equations. A typical example of the construction of a partial mesh in turbulent flows is shown in figure 3. The partial mesh contains the solid boundary of the airfoil as well as the wake of the flow field behind the trailing edge.

The local solution technique can be applied in combination with the zonal method for the solution of turbulent flow fields. Thus, there are two basic regions where the Euler and Navier-Stokes equations are solved respectively, while the local solution is applied in both these regions.

The construction of the inviscid and viscous regions in the zonal modelling are prescribed as input in the computational code. The local solution begins after a number of iterations on the fine mesh. The criterion for the beginning of the local solution procedure is an input value for the variation of the solution. This input value may be a value of the maximum variation of the conservative variables on the whole flow field.

In the present results a value for the variation max ($|\Delta(\varrho u)|$) has been used. When the numerical convergence meets this criterion then a partial mesh is constructed. The partial mesh contains all the numerical disturbances from the inviscid and viscous regions, which are larger than the convergence criterion. In the present calculations as convergence criterion has been considered, all the maximum variations of the conservative variables to be less than 10^{-5}.

The partial mesh of the local solution may overlap a part of the inviscid region and the whole viscous region, or only the viscous region. Partial meshes may be reconstructed during the numerical

solution. Each reconstruction of a partial mesh defines a local solution. In figures (3) and (4) two local solution levels are presented. In the first level the local solution overlaps a part of the inviscid region and all the viscous regions, while in the second level the partial mesh overlaps a part of the viscous region. The criterion for the construction of the local solution levels may be a prescribed number of iterations or a value of the numerical disturbances. After the convergence of the numerical solution on the partial mesh, it is not necessary to repeat the solution on the whole fine mesh, because the local solution does not influence the physics of the results.

Acceleration Strategy

The general solution procedure which is called multi-zonal local solution methodology, involves the mesh sequencing technique, the zonal modelling and the local solution of the equations. The zonal modelling, as well as the local solution of the equations, is applied only on the finest mesh of the solution. The steps of the acceleration strategy are the following :

a. Beginning of the numerical solution on the coarsest mesh.
b. Interpolation of the solution on the finer mesh, and repetition of the interpolations and the numerical solution up to the finest mesh.
c. Beginning of the numerical solution on the finest mesh using the zonal modelling.
d. Continuation of the iterations on the fine mesh up to the "meeting" with the criterion for the beginning of the local solution.
e. Beginning of the local solution and reconstruction, or not, of the partial meshes during the solution.

Step (e) is continued up to the steady state solution.

Turbulence modelling and multi-zonal local solution

The Baldwin-Lomax [10] algebraic turbulence model has been used for the present turbulent compressible flows. As we mentioned above, the partial mesh of the local solution may contain the viscous region, or the partial mesh may be a subset of the viscous region. In the first case eddy viscosity is calculated in the whole profile using the standard Baldwin-Lomax procedure. In the second case the functions of the turbulence model may be calculated either in the whole viscous region or in the partial mesh, which is a subset of this region.

In accordance with the Baldwin-Lomax turbulence model, eddy viscosity μ is given by

$$\mu_t = \begin{cases} (\mu_t)_{inner} & y \le y_1 \\ (\mu_t)_{outer} & y_v \ge y > y_1 \end{cases}$$

y_1 is the minimum normal distance from the wall at which values of the eddy viscosity in the inner and outer region are equal.
y_v is the normal distance from the wall at which the viscous zonal boundary or the local solution boundary are located.

The inner and outer regions are included into the viscous zonal boundary. The details of the Baldwin-Lomax model can be found in [10]. In the zonal methodology all the functions of the above model are calculated into the viscous region, while in the inviscid region the eddy viscosity is put equal to zero.

Results

The development of the multi-zonal local solution methodology has been obtained in transonic turbulent flows over a NACA 0012 airfoil. The first case concerns the flow with $M_\infty = 0.7$, a = 1.49 and $Re = 9 \times 10^6$. The results of computations have been compared with corresponding experimental results [11]. Two computational meshes with mesh size 120 x 30 and 240 x 60 (figs. 5a, b) have been used respectively. A physical image of the flow field is shown in figure 5c plotting the Iso-Mach lines. In figure 6 comparisons of the pressure coefficient distributions are presented. The comparison shows that the present results are in good agreement with the experimental data. The grid-dependent solution also shows that the differences between coarse and fine mesh results are small. The skin friction distribution for the coarse and the fine mesh are shown in figure 7. Skin friction is overestimated on the coarser mesh especially in the region around the leading edge.

Initially we tested the influence of the mesh sequencing procedure in the convergence behaviour. The calculations have been obtained for the fine mesh 240 x 60 using three mesh levels. The first level contains 60 x 15 grid points the second level 120 x 30, and the third level is the fine mesh with 240 x 60 grid points. Two cases of the mesh sequencing procedure have been tested. In the first case the calculations on the coarser meshes are continued up to the steady state solution on the coarser meshes and then the solution is interpolated to the fine mesh. In the second case the solution on the coarser meshes is interpolated on the fine mesh, but this solution is not the final steady state solution of the coarser meshes. The maximum variation of the conservative variables between two successive time steps is used as the convergence criterion. Comparisons of the convergence for the first and second case of the mesh sequencing procedure are presented in figure 8. The comparison shows that faster convergence is achieved when the coarse mesh solution is not the final steady state solution. It is proposed that as the convergence criterion on the coarser meshes the maximum variations of the conservative variables to be less or equal to 10^{-4}. The resutls for both cases are identical. This is shown on the figure for the pressure and the skin friction coefficient distributions.

In the above cases the mesh sequencing procedure has been used without zonal modelling and local solution of the equations. A significant increase of the algorithm efficiency is achieved when the multi-zonal local solution methodology is applied. In figure 9 are shown the convergence histories for three different solution cases. These cases are the solution on the fine mesh, the solution using the mesh sequencing procedure and the solution using the multi-zonal local solution

methodology. Considering as convergence criterion the maximum variation of the conservative variables to be equal to 8×10^{-6} the solution on the fine mesh requires about 4100 computational work units (CWU). Using the mesh sequencing procedure the solution requires about 2720 CWU while 1420 CWU are neccessary for the steady state solution using the multi-zonal local solution methodology. The most important contribution of the acceleration of the convergence is due to the local solution of the equations. The local solution of the equaitons is obtained in a small region of the fine mesh, including the viscous zonal boundary and the wake region. The results between the fine mesh solution and the multi-zonal local solution methodology are identical (figures 10a, b).

In order to reprove the behaviour of the multi-zonal local solution methodology on a coarser mesh, the calculations have also been repeated using a fine mesh of 120 x 30. Comparisons of the convergence histories are shown in figure 11. The multi-zonal local solution methodology (case 2, in fig. 11) increases the efficiency of the algorithm achieving faster convergence to the steady state solution than the mesh sequencing procedure and the fine mesh solution.

The convergence histories of figures 11 and 9 show that the efficiency of the multi-zonal local solution is greater when the number of computational points is increased. This is an important result because 3D complex calculations for engineering problems require a great number of grid points and significant computational cost and thus the multi-zonal local solution is expected to reduce significantly the computational cost.

A second flow case concerns the transonic turbulent flow around a NACA 0012 airfoil, with $M_\infty = 0.55$, $a = 8.34°$ and $Re = 9 \times 10^6$. In this flow case a shock wave is formed in the chordwise location $x/c = 0.1$. A physical picture of the flow field is shown in figure 12 plotting the Iso-Mach lines. The pressure coefficient and the skin friction coefficient distributions are shown in figures 13a, 13b for the fine mesh and the accelerated solution. In figure 13c comparison of the pressure coefficient distribution with the corresponding experimental data is presented. The results are in good agreement with the corresponding experimental results. The skin friction values indicate separation regions at the foot of the shock wave and at the region of the trailing edge, beginning at the $x/c = 0.72$ chordwise location [12].

The convergence behaviour has been tested for three different cases : 1. fine mesh solution. 2. Mesh sequencing procedure and zonal modelling and 3. multi-zonal local solution (mesh sequencing, zonal modelling and local solution). The convergence histories (fig. 14) justify the efficiency of the multi zonal local solution methodology for the present flow case where the shock wave and the separation region are formed. The computational cost is 1800 CWU using the multi-zonal local solution while 4700 CWU are needed using only the fine mesh. Comparison between case 2 and case 3 shows that the local solution is significantly responsible for the acceleration of the convergence, reducing by 200 CWU the convergence of case 3 in comparison with case 2.

Conclusions

The development of a multi-zonal local solution methodology for the accelerated solution of the Navier-Stokes equations in high Reynolds compressible flows is presented. The basic conclusions are as follows :

a. The multi-zonal local solution methodology reduces significantly the computational work units for the solution of the Navier-Stokes equations in high Reynolds compressible flows.

b. The accuracy of the results is not influenced by the accelerated procedure.

c. The local solution improves the classical mesh sequencing and zonal modelling as accelerated solution methods.

References

[1] Flares, J., Holst, T.L, Kaynak, U., Gundy, K.L., Thomas, S.D. : Transonic Navier-Stokes wing solution using a zonal approach : Part 1. Solution methodology and code validation. In : Application of computational fluid dynamics in aeronautics, AGARD CP 412, 1986.

[2] Van Dalsem, W.R., Steger, J.L. : Using the boundary-layer equations in three dimensional viscous flow simulation. In : Application of computational fluid dynamics in aeronautics, AGARD CP 412, 1986.

[3] Schmatz, M.A. : "Simulation of viscous flows by zonal solutions of the Euler, boundary-layer and Navier-Stokes equations, Z. Flugwiss. Weltraum-forsch., 11, 281-290, 1987.

[4] Schmatz, M.A., Mannager F., Wanie, K.M., : Numerical simulation of transonic wing flows using a zonal Euler, boundary-layer, Navier-Stokes approach. Z. Flugwiss, Weltraumforsch, 13, 377-384, 1989.

[5] Drikakis, D., Tsangaris, S. : Local solution acceleration method for the compressible Euler and Navier-Stokes equations, AIAA Journal, vol. 30/2, pp 340-348, 1992.

[6] Drikakis, D. : Development of upwind computational methods for the high speed aerodynamics, Ph. D. thesis National Technical University of Athens, 1991.

[7] Steger, J.L., Warming R.F. : Flux vector splitting of the inviscid gas dynamic equations with applicaiton to finite difference methods, J. Comp. Phys., vol. 40, 263-293, 1981.

[8] Chakravarthy, S.R. : High resolution upwind formulations for the Navier Stokes equations, VKI Lecture Series Comp. Fluid Dynamics, 1988-05, 1988.

[9] Drikakis, D., Tsangaris, S. : Laminar and turbulent viscous compressible flows using improved flux vector splittings, 9th GAMM Conference on Numerical methods in Fluid Mechanics, Lausanne, Sept. 1991.

[10] Baldwin, B.S., Lomax H. : Thin layer approximation and Algebraic Model for separated turbulent flows, AIAA paper 78-257, AIAA 16th Aerospace Sciences Meeting, Huntsville, Alabama, Jnauary 16-18, 1978.

[11] Harris, C.D. : Two dimensional aerodynamics characteristics of the NACA 0012 airfoil in the Langley 8-Foot Transonic Pressure Tunnel, NASA TM 81927, 1981.

[12] Coakley, T.J. : "Numerical simulation of Viscous Transonic Airfoil Flows", AIAA 87-0416, AIAA 25th Aerospace Sciences Meeting, Jan. 12-15, 1987 Reno, Nevada.

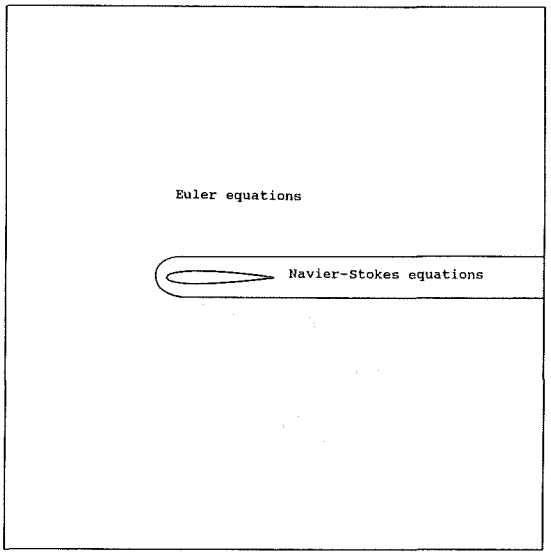

Fig.1 : The scheme of zonal modelling.

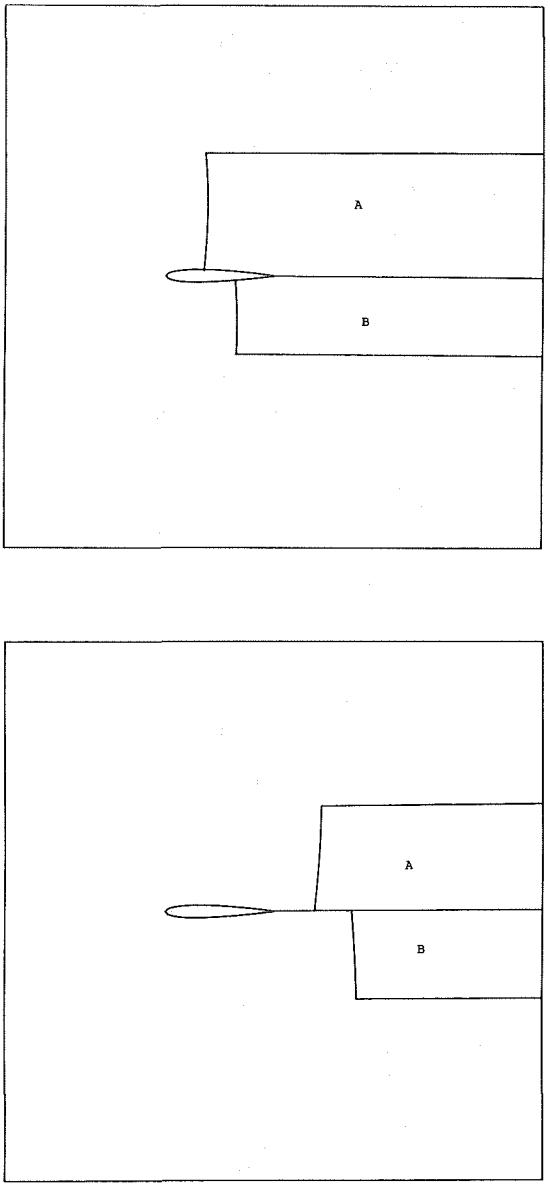

Fig.2 : Subregions for the local adaptive solution (typical examples).

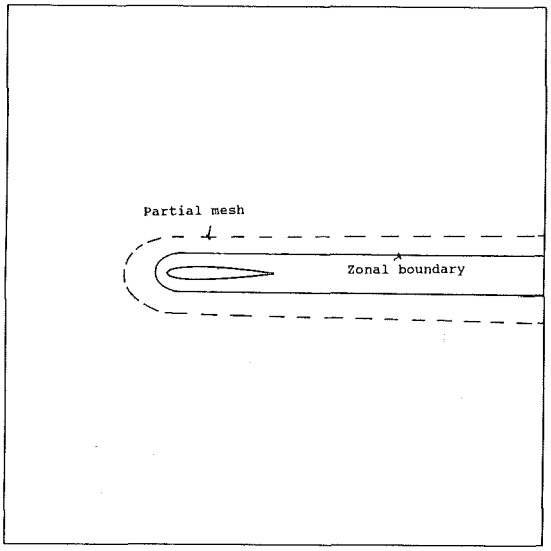

Fig.3 : Construction of the partial mesh, overlaping a part of inviscid region and all the viscous regions. (first level).

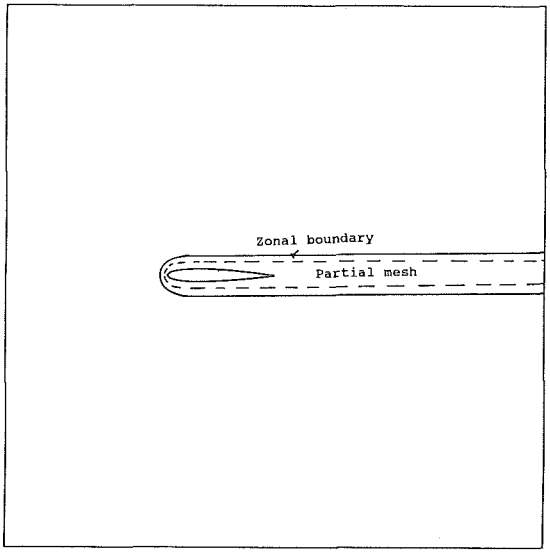

Fig.4 : Construction of the partial mesh, overlaping a part of the viscous region (second level).

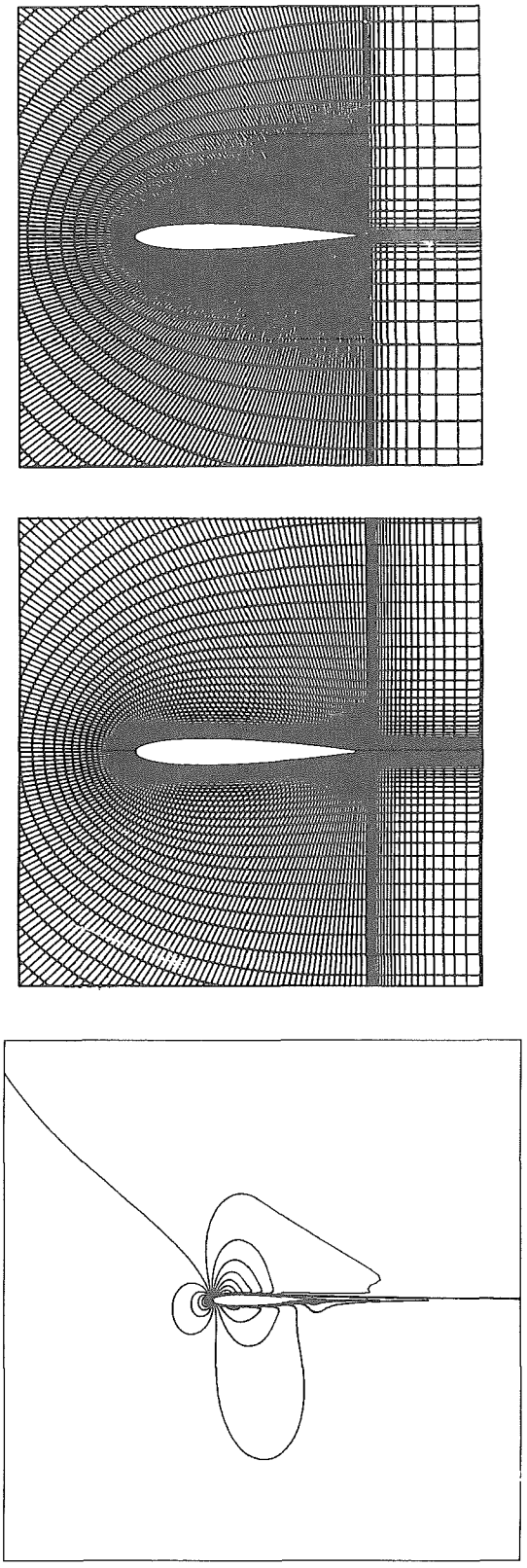

Fig.5 : Computational meshes around a NACA-0012 airfoil : a) meshsize : 120 x 30, b) meshsize : 240 x 60 c) Iso-Mach lines of the flow field (M_∞ = 0.7, a = 1.49 deg, Re = $9 \cdot 10^6$).

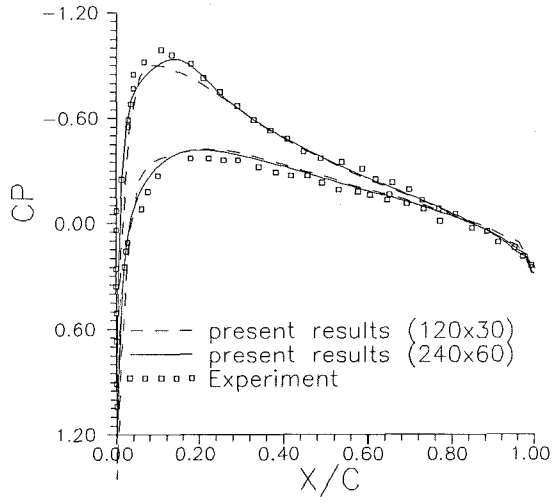

Fig.6 : Pressure coefficient distribution and comparison with experiments. (M_∞= 0.7, a = 1.49 deg., Re = $9 \cdot 10^6$, NACA-0012 airfoil).

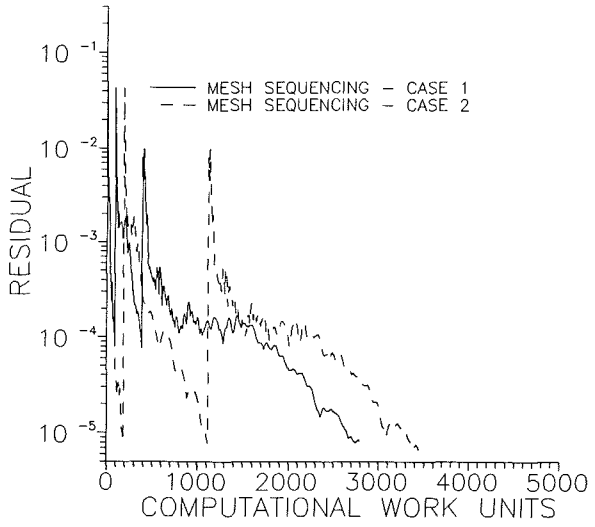

Fig.8 : Comparison of the convergence histories for two different mesh sequencing procedures.

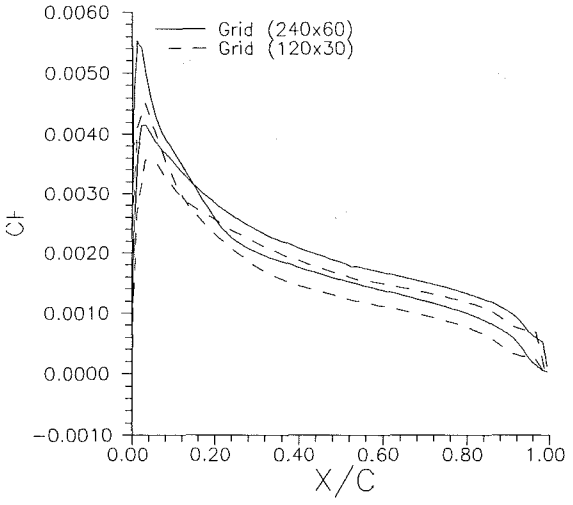

Fig.7 : Skin friction coefficient (M_∞= 0.7, a = 1.49 deg, Re = $9 \cdot 10^6$, NACA-0012 airfoil).

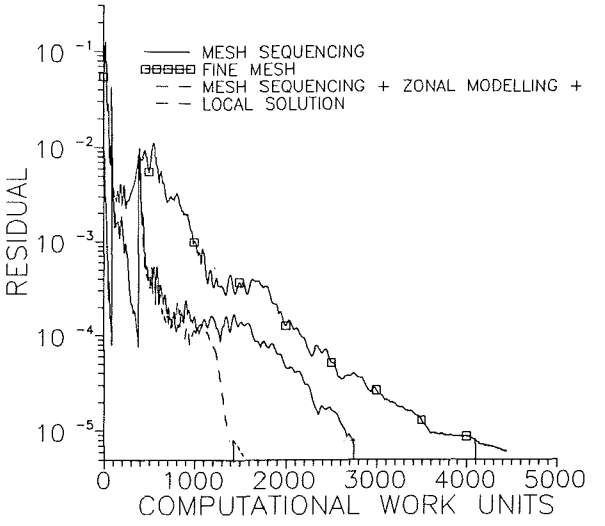

Fig.9 : Comparison of the convergence histories for three different solution cases.
(NACA-0012, M_∞ = 0.7, a = 1.49 deg, Re = $9 \cdot 0^6$).

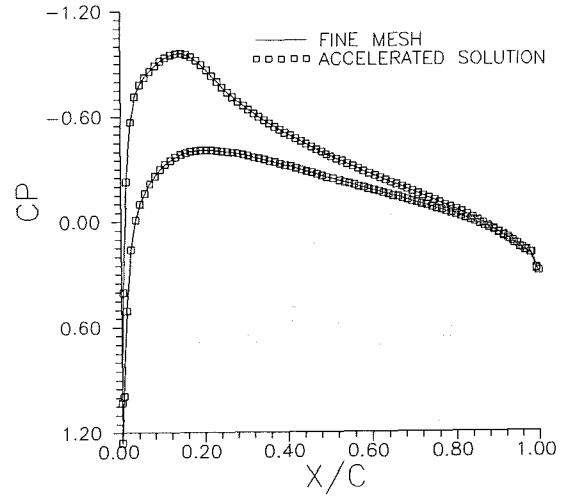

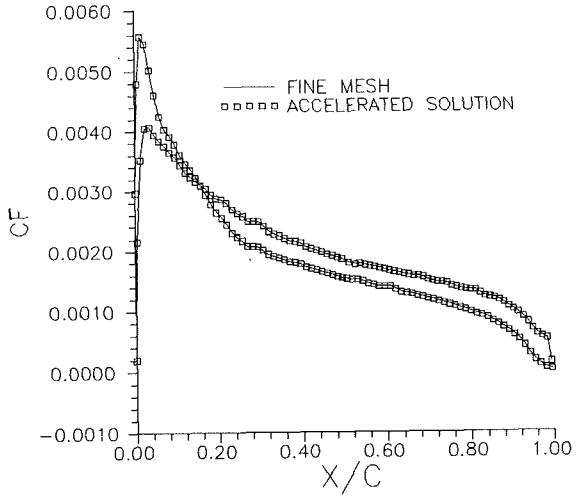

Fig.10 : Comparison between the fine mesh and multizonal local solution methodology (NACA-0012, M_∞ = 0.7, a = 1.49 deg, Re = $9 \cdot 10^6$) :
a. Pressure coefficient
b. Skin friction coefficient.

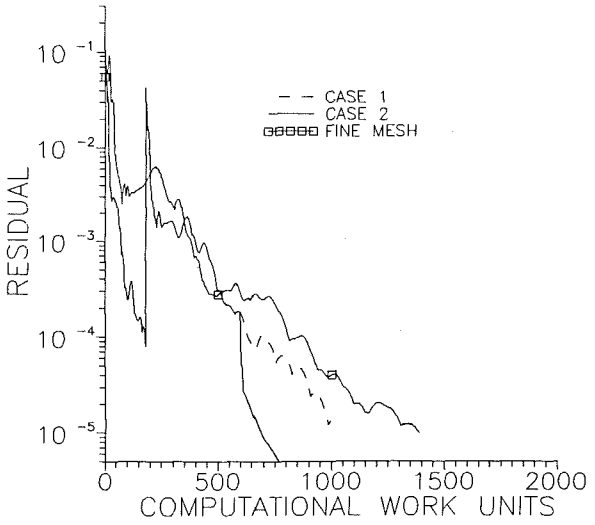

Fig.11 : Comparison of the convergence histories.
case 1 : Mesh sequencing procedure
case 2 : Multizonal local solution methodology
Fine mesh solution (grid 120 x 30)
(NACA 0012, M_∞ = 0.7, a = 1.49 deg, Re = $9 \cdot 10^6$).

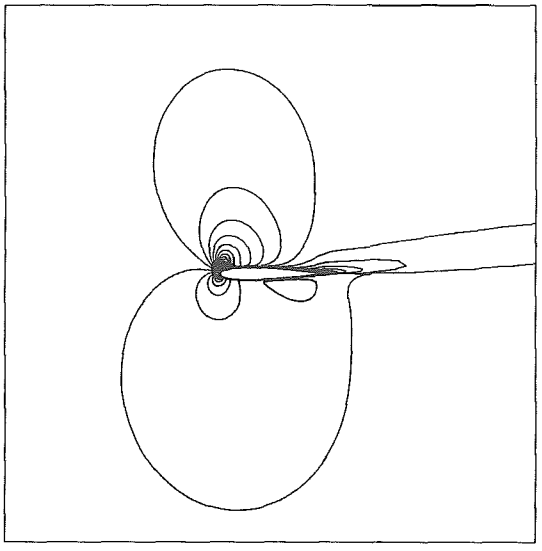

Fig.12 : Iso-Mach lines of the flow around a NACA-0012 airfoil (M_∞ = 0.55, a = 8.34°, Re = $9 \cdot 10^6$).

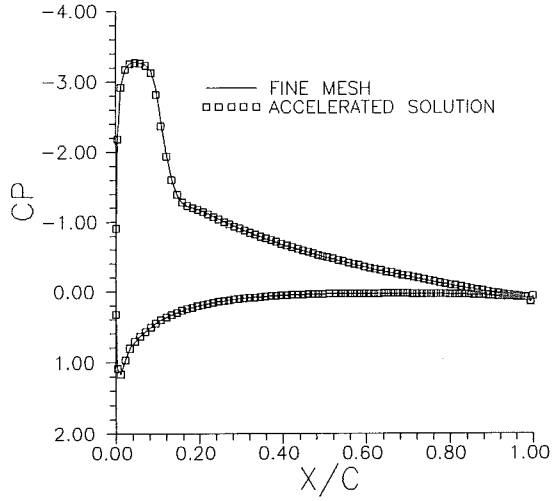

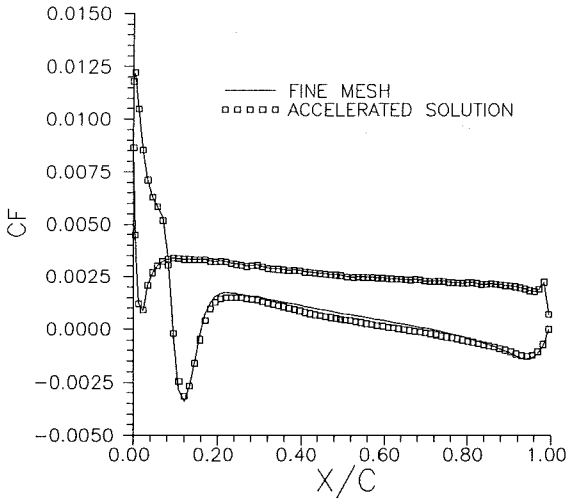

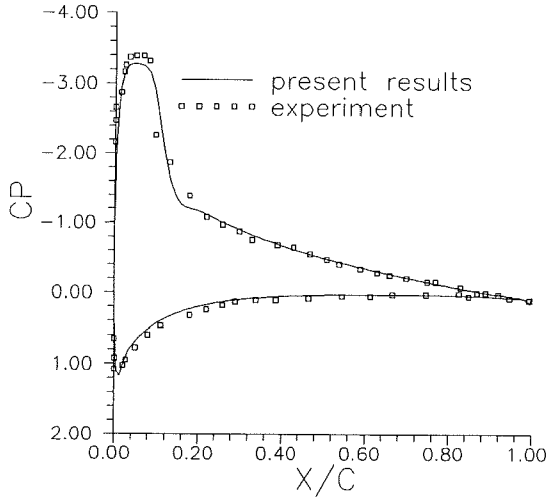

Fig.13 : Comparison of the fine mesh and accelerated solution :
a. Pressure coefficient
b. Skin friction coefficient.
c. Comparison of the pressure coefficient for the accelerated solution with experimental results [11].

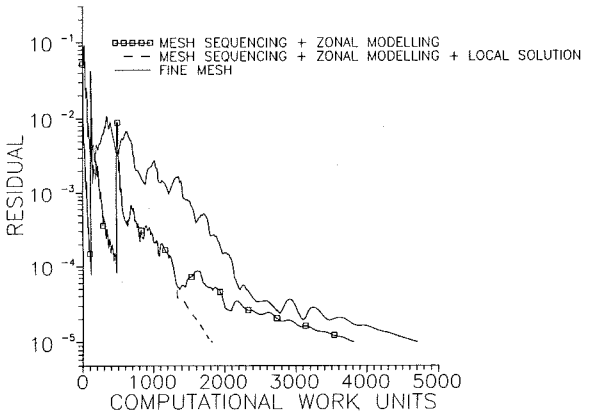

Fig.14 : Comparison of the convergence histories for three different solution cases. (NACA-0012, M_∞ = 0.55, a = 8.34°, Re = $9 \cdot 10^6$).